https://doi.org/10.1038/s44407-025-00011-y

Impacts of dimethylamine emissions on particle number concentration and cloud condensation nuclei in Beijing

Zhicheng Feng[1], Jianjiong Mao[2], Lei Jiang[1], Yanjie Qian[1], Dongjie Shang[2], Song Guo[2], Min Hu[2] & Jianlin Hu[1] ✉

New particle formation (NPF) is a key source of atmospheric particles and cloud condensation nuclei (CCN). In polluted regions, the nucleation mechanism of sulfuric acid (H_2SO_4)-dimethylamine (DMA) is thought to play a crucial role in NPF. However, it still remains unclear about the sources of DMA and their contributions to regional particle number concentrations (PNC) and CCN. In this study, we incorporated the H_2SO_4-DMA nucleation mechanism into the aerosol module in the WRF-Chem model to improve the model's simulation ability for NPF events. The default 8 size bins covering 39 nm to 10 μm were extended to 12 size bins ranging from 1 nm to 10 μm to better capture the formation and growth of the small particles. The modified model was applied to Beijing and its surrounding areas for an observation episode from March 1 to 18 in 2017. The results show that the revised model significantly improves its capability in simulating the particles number in the smaller size range (<20 nm), reducing the standardized bias from over 58% to 10%. The H_2SO_4-DMA nucleation mechanism contributes 46–78% of PNC in the surface layer (from the surface to ~300 m) and 22–36% of CCN at 0.5% supersaturation ($CCN_{0.5\%}$). The contributions to PNC and $CCN_{0.5\%}$ are notably higher on NPF days than those on non-NPF days. High PNC zones correspond to areas with elevated $CCN_{0.5\%}$, suggesting that the nucleation process leads to increased CCN concentrations, and these regions also exhibit higher levels of H_2SO_4 and DMA. Agricultural and residential activities were identified as the main sources of DMA in the study area. The contribution of residential DMA to PNC is particularly significant in urban Beijing, reaching up to 70%. This study enhances our understanding of how NPF events induced by H_2SO_4-DMA nucleation affect PNC and CCN in intensive anthropogenic emission regions.

New particle formation (NPF) refers to the process that gaseous vapors form stable molecular clusters and then undergo condensation and coagulation growth to become particles[1,2]. NPF can contribute greatly to particle number concentration (PNC)[3], and the generation of ultrafine particles poses potential threats to human health[4]. When newly generated particles grow to a certain size (diameter >60 nm), they can be activated to become cloud condensation nuclei (CCN) under actual supersaturated conditions[5], which affects the cloud properties, and thus indirectly influences the atmospheric radiation balance and climate change[6–8]. In addition, NPF and subsequent growth of particles can lead to severe air pollution[9,10].

NPF has been recognized as a significant source of both PNC and CCN in various environments[11–15]. In regions like the Amazon rainforest, where anthropogenic pollution is minimal, organic nucleation plays a dominant role. During the rainy season, NPF within the boundary layer can contribute approximately 90% of PNC and 80% of CCN[15]. Yu et al.[14] found that PNC and CCN concentrations increased rapidly during winter NPF events in the northeastern United States, with nucleation contributing up to 85% of PNC

[1]Jiangsu Key Laboratory of Atmospheric Environment Monitoring and Pollution Control, Collaborative Innovation Center of Atmospheric Environment and Equipment Technology, School of Environmental Science and Engineering, Nanjing University of Information Science & Technology, Nanjing, 210044, China. [2]State Key Joint Laboratory of Environmental Simulation and Pollution Control, College of Environmental Sciences and Engineering, Peking University, 100871 Beijing, China. ✉e-mail: jianlinhu@nuist.edu.cn

near the surface and 20–50% of CCN. Matsui et al.[12] suggested that NPF contributed approximately 20–30% to PNC during the study period and significantly increased CCN concentrations at supersaturations greater than 0.2% in Beijing and its surrounding regions.

Nucleation is considered the first step in the process by which gaseous vapors are converted into stable molecular clusters, eventually leading to particle formation in NPF. Due to its extremely low saturation vapor pressure, gaseous sulfuric acid (H_2SO_4) is regarded as one of the most important precursors in the nucleation process[16–18]. Besides H_2SO_4, other precursors have been identified to play important roles in nucleation, including ammonia (NH_3)[19], nitric acid (HNO_3)[20], oxidized organic vapors[21], iodine oxides[22], and dimethylamine (DMA)[23]. In recent years, intense NPF events have been frequently observed in polluted urban areas. Research shows that H_2SO_4-DMA clusters can effectively explain the high frequency of NPF in such environments[24], and growing evidence supports the role of the H_2SO_4-DMA nucleation mechanism in driving these intense NPF events[25–27]. Experimental studies have shown that compared to NH_3, which is also an alkaline gas, DMA can increase the new particle formation rate by a factor of 1000 when concentrations exceed 3 ppt, even though NH_3 emissions are much higher than those of DMA in the atmosphere[28,29].

Early studies identified agricultural sources (primarily livestock) as the main contributors of DMA[28]. However, observations in suburban Nanjing have shown that industrial sources might be the primary contributors of DMA in that area[30]. Additionally, Mao et al.[31] found that DMA emissions in the Yangtze River Delta primarily originate from agricultural and residential sources. A recent mobile observation studies[32] suggest that average DMA concentrations in urban areas are higher than in rural regions, indicating that agricultural sources may no longer be the dominant contributors in cities. Therefore, emissions of non-agricultural DMA sources in urban areas require increased attention.

Despite the growing evidence that H_2SO_4-DMA nucleation is a key mechanism for NPF in urban environment and anthropogenic emissions are important DMA sources in urban environments, understanding about the impacts of DMA emissions on PNC and CCN remain limited. The objective of this study is to incorporate the H_2SO_4-DMA nucleation mechanism into regional chemical transport model to quantify its specific effects on PNC and CCN. In this study, we incorporated the DMA chemistry as well as the H_2SO_4-DMA nucleation mechanism into the WRF-Chem model with modifications in the MOSAIC aerosol module. We then applied the revised model to simulate NPF events during an observation episode from March 1 to March 18, 2017 in Beijing and its surrounding areas. We further analyzed the contributions of different DMA sources to PNC and CCN.

Results

Model validation

The modified WRF-Chem model incorporating the H_2SO_4-DMA nucleation mechanism was evaluated under three scenarios, with detailed explanations of each scenario provided in the Methods section. In the 8bin-modified model, a comparison between simulated and observed particle number size distribution (PNSD) showed that the results from the sim_no, sim_default, and sim_DMA scenarios were similar, all substantially overestimating particle number concentrations below 100 nm by more than 67% (Supplementary Fig. 1). The model also failed to accurately capture particle number concentrations across different size ranges, which may be attributed to the relatively coarse size resolution of the 8bin-modified model[33]. After increasing the number of size bins, Fig. 1a shows the comparison of simulated and observed PNC in different size ranges in the 12bin-modified model. The simulations from both the sim_no and sim_default scenarios were approximately an order of magnitude lower than the observed average PNSD in the 3–20 nm size range. Specifically, the observed average number concentration was 9859 cm^{-3}, while the simulated average number concentrations from sim_no and sim_default were 1916 and 4060 cm^{-3}, respectively, both exhibiting significant underprediction (Fig. 1b). After incorporating the H_2SO_4-DMA nucleation mechanism into the model, the simulated average PNSD in the 3–20 nm range exhibited improved agreement with observational data, resulting in an average number concentration of 9491 cm^{-3} within this size range. This adjustment reduced the normalized deviation to below 10%. The introduction of this mechanism brought the simulation results of PNSD in line with those of Li et al.[34]. The inclusion of the H_2SO_4-DMA nucleation mechanism significantly improved the model's accuracy in simulating number concentrations for smaller particles, indicating the crucial role of DMA in the nucleation process.

In the time series of PNSD, NPF events were identified based on a rapid increase in observed particle number concentration in the 3–10 nm size range, with concentrations exceeding 10^4 cm^{-3} [35–37]. As shown in Fig. 1c, a total of nine NPF events were recorded during the observation period, and days on which NPF events occurred were classified as NPF days. During these days, a characteristic burst in nanoparticle number concentrations followed by subsequent growth was observed. Fig. 1d shows that the model using the default binary nucleation mechanism failed to reproduce the explosive growth of particle number concentrations in the 3–10 nm size range on three selected NPF days (i.e., March 1, March 9, and March 14). Incorporating the H_2SO_4-DMA nucleation mechanism successfully captured the sharp increase in particle number concentrations in the 3–10 nm size range on these days. In contrast, for the remaining six NPF events, except for March 11, the incorporation of the H_2SO_4-DMA nucleation mechanism also successfully reproduced the rapid increase in particle number concentrations in the low size range, as well as the subsequent growth processes on the other five NPF days (Supplementary Figs. 2 and 3). This result suggests that the H_2SO_4-DMA nucleation mechanism may be the primary driver of NPF events during the observation period. The model did not reproduce the NPF events on March 11, likely due to that other nucleation mechanisms, such as organics involved nucleation processes, might contribute importantly on this day but were not considered in this study. A number of studies have revealed that organic compounds also play an important role in the nucleation process and the H_2SO_4-organic nucleation mechanism can explain certain NPF events in urban areas of China[38–41].

Meteorological parameters and concentrations of other species were also validated. Meteorological factors play a role in NPF events, with wind speed, for example, affecting the concentration of precursor gases and the condensation sink[1]. The evaluation of simulated meteorological parameters for the period from March 1 to 18, 2017, is shown in Supplementary Table 1, where the mean bias (MB), mean error (ME), root mean square error (RMSE), and index of agreement (IOA) are calculated and summarized. The MB, RMSE, and IOA for simulated wind speed at 10 m (WS10) are 0.24 m s^{-1}, 1.52 m s^{-1}, and 0.76, respectively, while the MB, ME, and IOA for specific humidity are 0.03 g kg^{-1}, 0.43 g kg^{-1}, and 0.87, respectively. Both are within the benchmark recommended by Emery and Tai[42] and Tesche[43]. Additionally, the model slightly underestimated the air temperature at 2 m (T2). Overall, the model performed well in capturing the variations in meteorological fields during the analysis period.

The model's simulation results for SO_2 and $PM_{2.5}$ related to NPF were validated and analyzed. The results show that the model slightly underestimated the hourly concentrations of $PM_{2.5}$ and SO_2 compared to observations, with normalized mean biases (NMB) of −0.45 and −0.38, respectively (Supplementary Fig. 4). However, the correlation between the simulated and observed data was strong, with correlation coefficients of 0.75, both within the benchmark recommended by Emery et al.[44]. For the two key precursors of H_2SO_4-DMA nucleation, H_2SO_4 and DMA, although there were no observational data available for this period, the simulations showed an average H_2SO_4 concentration of 10^7 cm^{-3} and an average DMA concentration of 2.98 ppt. These simulated concentrations of H_2SO_4 and DMA are consistent with other studies using the WRF-Chem model and fall within reasonable simulation ranges[31,34,36,45].

Contributions of H_2SO_4-DMA Nucleation to PNC and CCN

In the sim_all scenario, the contributions of different nucleation mechanisms and primary emissions to PNC and CCN were compared. The

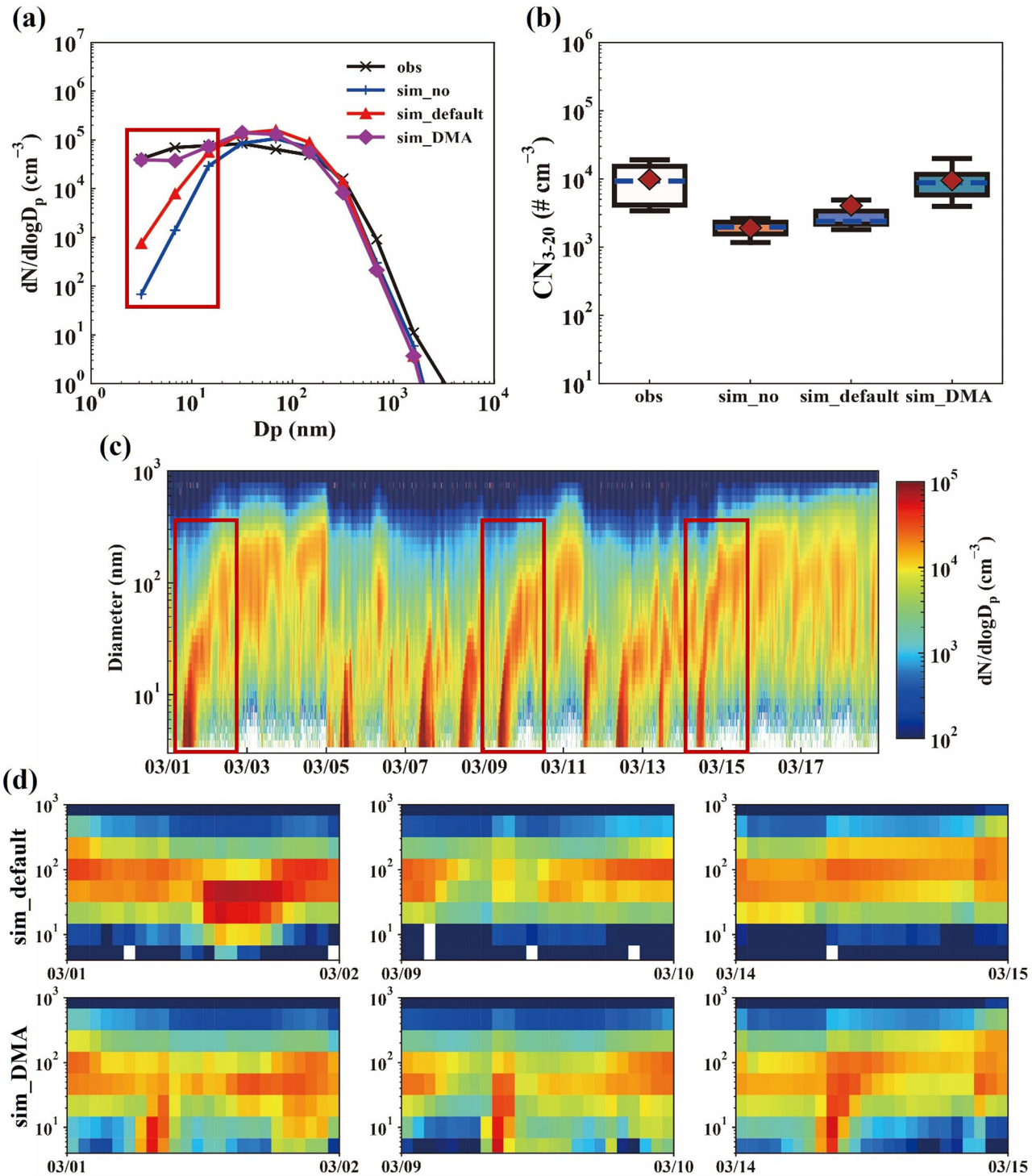

Fig. 1 | Comparison of simulation results under different nucleation scenarios with observations from March 1 to 18, 2017. Averaged particle number size distribution simulated and observations (**a**). Box plot showing a comparison of simulated and observed number concentrations for particles in the 3–20 nm size range (**b**). Time series of observed particle number size distributions (**c**). Simulated particle number size distributions using the default nucleation mechanism and the H_2SO_4-DMA nucleation mechanism on March 1, March 9, and March 14 (**d**).

simulation result for number concentrations under this scenario is shown in Supplementary Fig. 5. Below approximately 300 m near the surface, the H_2SO_4-DMA nucleation mechanism dominates (Fig. 2a), primarily due to the higher concentration of DMA near the surface, which decreases with altitude (Supplementary Fig. 6), as well as the relatively short atmospheric lifetime of DMA[46]. Above 300 m, nucleation involving NH_3 becomes the primary pathway. Studies at the urban Beijing site have similarly found that H_2SO_4-DMA nucleation is the dominant mechanism, contributing to more than 60% of PNC[34]. Recent research also indicates that in densely populated areas of eastern China, India, Europe, and parts of the United States, H_2SO_4-DMA nucleation plays a leading role near the surface[47]. Within the altitude range where H_2SO_4-DMA nucleation is dominant, this mechanism contributes 46–78% to PNC and 22–36% to CCN at 0.5% supersaturation ($CCN_{0.5\%}$). However, the relative importance of H_2SO_4-DMA nucleation

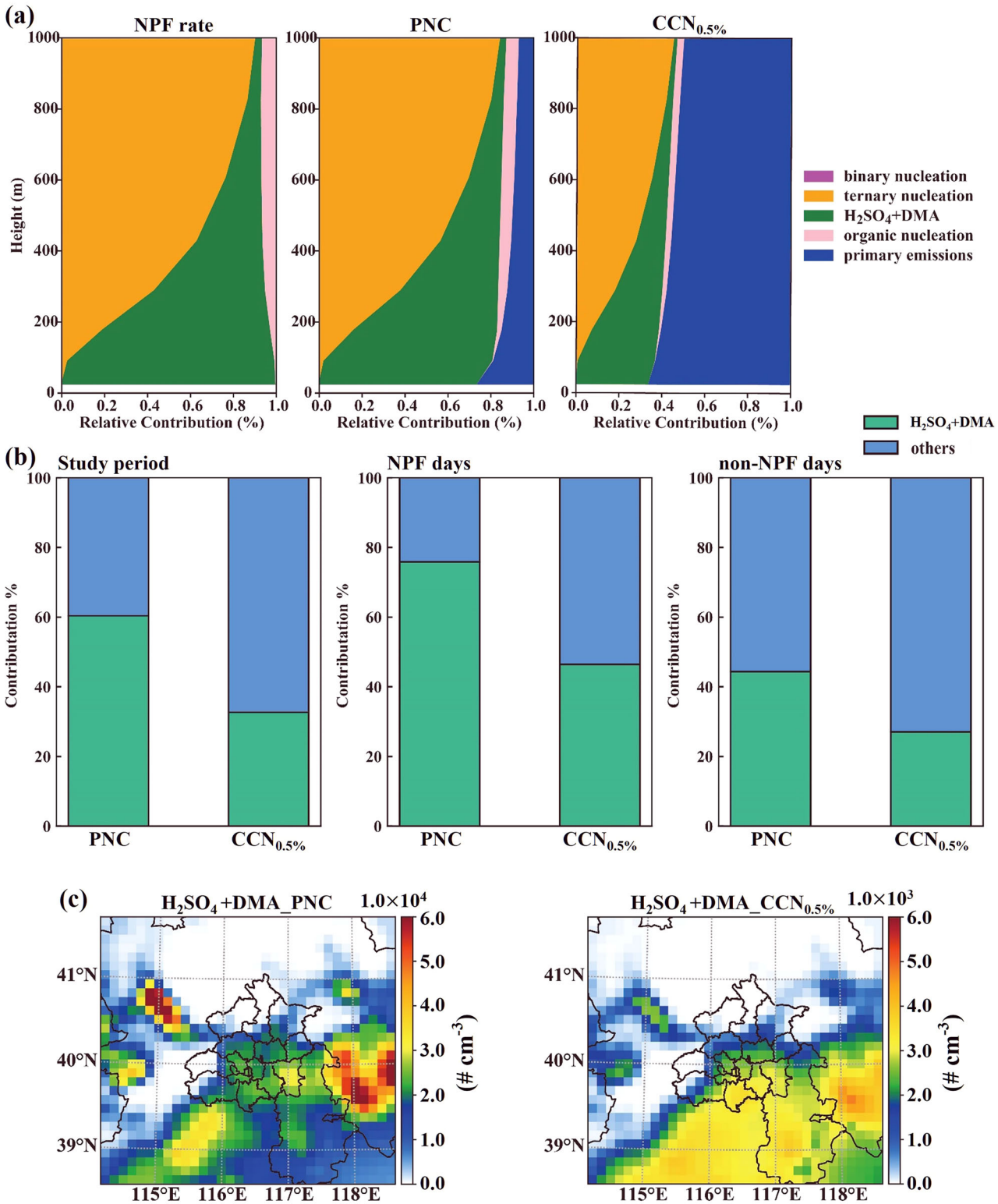

Fig. 2 | Contributions of H_2SO_4-DMA nucleation-induced NPF to PNC and $CCN_{0.5\%}$. Comparison of different nucleation mechanisms and their relative contributions to PNC and $CCN_{0.5\%}$ within the study area (**a**). Contributions of H_2SO_4-DMA nucleation to PNC and $CCN_{0.5\%}$ at the Beijing site: overall contributions, and relative contributions on NPF and non-NPF days (**b**). Spatial distribution of the average PNC and $CCN_{0.5\%}$ generated by H_2SO_4-DMA nucleation near the surface (**c**).

and its contributions to PNC and $CCN_{0.5\%}$ decrease as altitude increases. When considering the impact of primary emissions on PNC and $CCN_{0.5\%}$, primary emissions contribute up to 26% to PNC near the surface, but this influence weakens with altitude. For $CCN_{0.5\%}$, primary emissions dominate within the 1 km range near the surface, contributing 49-65%. Particles formed through H_2SO_4-DMA nucleation need to grow to reach the size required for activation as $CCN_{0.5\%}$. In contrast, particles from primary emissions are often already large enough to be activated. As a result, primary emissions have a greater influence on $CCN_{0.5\%}$ near the surface. Overall, within the 300-meter altitude range near the surface, the H_2SO_4-DMA

nucleation mechanism is the primary source of PNC compared to other nucleation mechanisms and primary emissions. Although its impact on $CCN_{0.5\%}$ is smaller than that of primary emissions, it remains significant and should not be overlooked.

Based on the results of the sim_all scenario, the average contributions of H_2SO_4-DMA nucleation to PNC and $CCN_{0.5\%}$ were approximately 60% and 32% respectively (Fig. 2b) during the entire study period. The contributions of H_2SO_4-DMA nucleation to PNC and CCN on NPF days were 31% and 19% higher than on non-NPF days, respectively. On NPF days, the PNC driven by H_2SO_4-DMA nucleation was markedly higher than that on non-NPF days (Supplementary Fig. 7). On non-NPF days, the contributions of H_2SO_4-DMA nucleation to PNC and $CCN_{0.5\%}$ were lower than the average levels observed throughout the study period, suggesting that the increase in PNC and $CCN_{0.5\%}$ due to H_2SO_4-DMA nucleation primarily occurred on NPF days. Previous studies at the Beijing site have also noted that nucleation processes exert a more pronounced impact on PNC and CCN during NPF days[12]. Overall, H_2SO_4-DMA nucleation significantly contributed to both PNC and $CCN_{0.5\%}$ on both NPF and non-NPF days, with its impact being particularly pronounced on NPF days.

Figure 2c shows the regional distributions of H_2SO_4-DMA contributed PNC and $CCN_{0.5\%}$ in the modeling domain. High PNC regions generated by H_2SO_4-DMA nucleation closely correspond with the high $CCN_{0.5\%}$ regions, primarily concentrated in southern Beijing, eastern Hebei, and areas to the west and south of Beijing. In these regions, the PNC and $CCN_{0.5\%}$ values can reach 20,000 cm^{-3} and 2000 cm^{-3}, respectively, and in some areas even as high as 50,000 cm^{-3} and 4000 cm^{-3}. This suggests that particles generated by H_2SO_4-DMA nucleation may have contributed to the increase in $CCN_{0.5\%}$. The contributions of H_2SO_4-DMA nucleation to PNC and $CCN_{0.5\%}$ can exceed 40% and 20%, respectively (Supplementary Fig. 8). Additionally, primary emissions in these areas also contributed significantly to PNC and $CCN_{0.5\%}$ (Supplementary Fig. 9), as reflected in the sim_no scenario. While primary emissions contributed less to PNC than nucleation processes, they contributed more to $CCN_{0.5\%}$.

In regions where high PNC and $CCN_{0.5\%}$ values are generated by H_2SO_4-DMA nucleation, higher concentrations of DMA are often observed (Supplementary Fig. 10a). In urban Beijing, although the highest DMA concentrations exceed 4 ppt, the corresponding concentrations of H_2SO_4 vapor and its precursor SO_2 are lower compared to other high-value regions (Supplementary Fig. 10b, c), which inhibits the formation of larger and more stable clusters[27]. Moreover, when the H_2SO_4 concentration is $\leq 3 \times 10^7$ cm^{-3} (1.2 ppt), the threshold DMA concentration for nucleation rates is typically around 5 ppt, and further increases in DMA concentration do not significantly accelerate nucleation rates in the environment[24,29]. Due to these factors, the PNC and $CCN_{0.5\%}$ produced by nucleation in urban Beijing are not higher than in the surrounding areas. In eastern Hebei, both DMA and H_2SO_4 vapor concentrations are high, which leads to higher PNC and $CCN_{0.5\%}$ values from H_2SO_4-DMA nucleation compared to other simulated regions, with more significant contributions to both.

Contributions of different DMA sources in H_2SO_4-DMA nucleation

The emission inventory estimated for DMA in this study show that agricultural sources are the largest contributor to DMA in the study area, accounting for approximately 58%, while residential sources are another major contributor, with a share of around 37% (Supplementary Fig. 11a). This finding is consistent with the Yangtze River Delta region, where agriculture and residential sources are also the main contributors to amine emissions, contributing approximately 66% and 31% to the regional average amine levels, respectively[31]. Spatially, the simulation results show that agricultural DMA emissions are mainly distributed in eastern Hebei and areas south of Beijing during the study period, with an average concentration of approximately 2.2 ppt (Supplementary Fig. 11b). In contrast, residential DMA emissions are concentrated around urban Beijing, with an average concentration of approximately 2.7 ppt, and there are also higher residential DMA emissions south of Beijing (Supplementary Fig. 11c). Based on the dominance and spatial distribution of agricultural and residential sources of DMA, the specific impact of these two sources during H_2SO_4-DMA nucleation was further quantified.

Figure 3 shows the impact of agricultural and residential DMA emissions on PNC. In the entire study area, agricultural sources of DMA contribute approximately 52% of PNC in H_2SO_4-DMA nucleation, while residential sources contribute about 13%. In urban Beijing, where residential DMA emissions are concentrated, residential sources account for up to 78% of the PNC (Fig. 3a). High PNC values caused by agricultural DMA emissions spatially correspond to the high DMA concentration areas from agricultural sources (Supplementary Fig. 12a). In eastern Hebei, where both agricultural DMA emissions and nucleation precursor H_2SO_4 concentrations are high (Supplementary Fig. 10b), the PNC values resulting from agricultural DMA nucleation are the highest in the entire study area, averaging around 25,000 cm^{-3}. In areas south of Beijing, although agricultural DMA emissions are comparable to those in eastern Hebei, the concentration of the nucleation precursor H_2SO_4 is significantly lower. As a result, the PNC values from agricultural DMA involved in H_2SO_4-DMA nucleation are lower in southern Beijing compared to eastern Hebei. In terms of spatial distribution, agricultural DMA contributes to over 40% of the total PNC generated by H_2SO_4-DMA nucleation, except in areas near urban Beijing (Fig. 3b). The spatial distribution of PNC changes driven by residential DMA emissions corresponds closely to the distribution of residential DMA itself (Supplementary Fig. 12b). The proportion of PNC generated by H_2SO_4-DMA nucleation involving residential DMA near urban Beijing is notably higher than in other areas, reaching around 70%. A similar situation is observed in urban Shanghai, where residential DMA emissions are the main driver of particle formation, accounting for 78% and 68% of total PNC in July and December, respectively[32]. Based on studies conducted in Beijing and Shanghai, two densely populated megacities, the impact of residential DMA emissions on particle number concentrations in urban areas has been revealed. Therefore, reducing residential DMA emissions may become an effective strategy for controlling ambient particle number concentrations in urban China, offering multiple benefits for air quality, human health, and climate change mitigation. The findings presented in the earlier sections of this study indicate that the spatial distribution of $CCN_{0.5\%}$ corresponds to that of PNC, suggesting that the influence of DMA from different sources on $CCN_{0.5\%}$ during nucleation may be consistent with its effect on PNC.

Discussion

Incorporating the H_2SO_4-DMA nucleation mechanism into the model significantly improved its ability to simulate NPF and highlighted this mechanism as the primary driver of NPF events in the Beijing region. Consistent with previous studies that identified H_2SO_4-DMA nucleation as dominant in human-polluted environments[34,48,49], we further quantified the impact of this mechanism on PNC and CCN. Based on the emission inventory and simulation results, we found that agriculture and residential sources are the main contributors to DMA, with residential sources playing a particularly significant role in urban areas. Moreover, DMA emissions from residential sources participating in H_2SO_4-DMA nucleation substantially contribute to urban PNC, providing a more reliable basis for attributing CCN and aerosol radiative forcing in urban areas to specific sources.

However, due to the lack of long-term and continuous observations of DMA and CCN, it is currently not possible to comprehensively evaluate the simulation performance of the model. We acknowledge that uncertainties remain in the representation of DMA sources and sinks, as well as in the nucleation parameterization when simulating H_2SO_4-DMA nucleation in the model. The lack of heterogeneous reactions associated with H_2SO_4 in MOSAIC aerosol module introduces corresponding uncertainties for H_2SO_4, another key precursor of nucleation. The absence of observational data further complicates the accurate evaluation of the simulation results for H_2SO_4. Additionally, aerosol particle size distribution is another source of uncertainty in the model. Although the size bins have been increased from 8

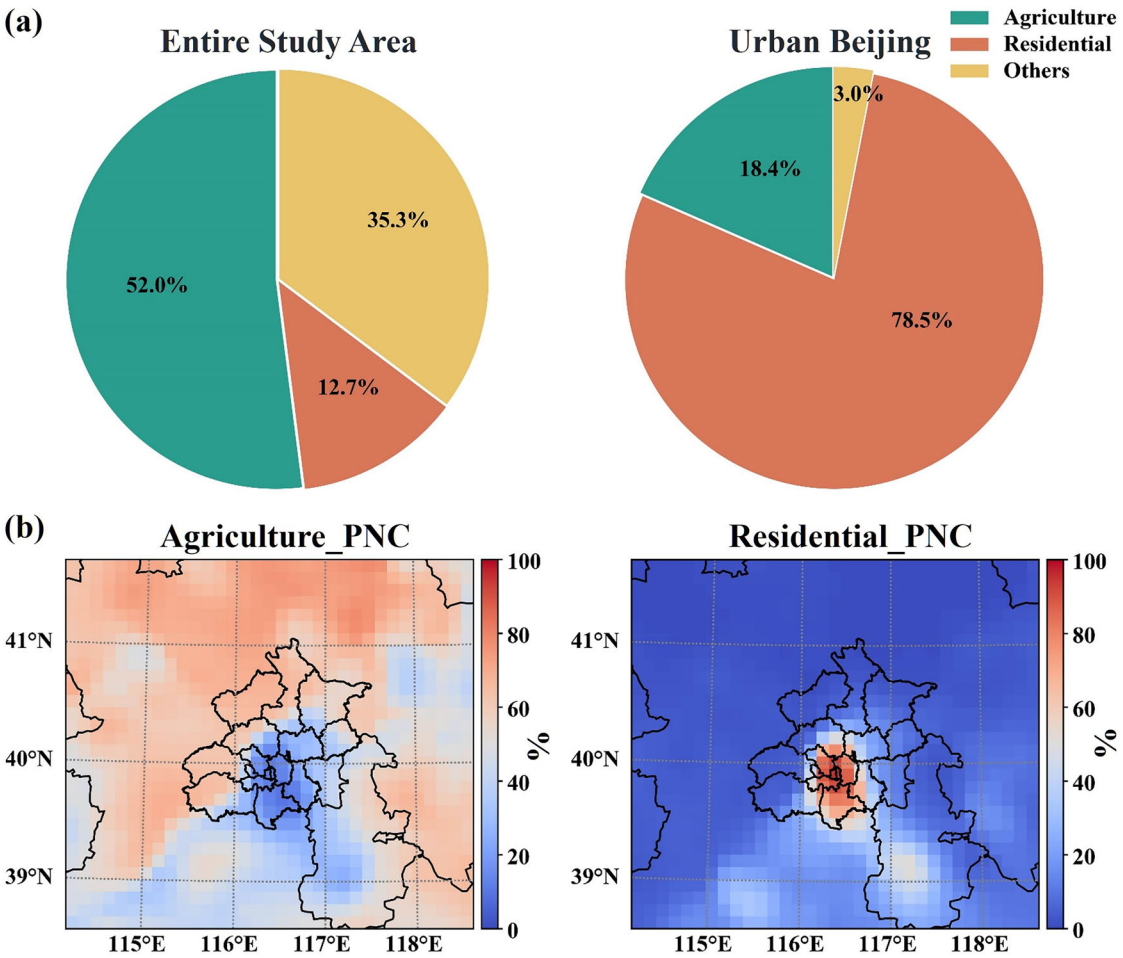

Fig. 3 | Contributions of different DMA sources in H_2SO_4-DMA to PNC. Contributions of different DMA sources in the entire study area and urban Beijing (**a**). Spatial distribution of PNC proportion attributed to agricultural and residential sources relative to total PNC near the surface (**b**).

to 12, the resolution of the particle size remains insufficiently detailed. These uncertainties highlight the need for further research to address these limitations.

Methods

Model development

We employed the WRF-Chem model version 3.9[45,50,51] to investigate the impacts of DMA emissions on NPF events and contributions to PNC and CCN. DMA emissions and chemistry was added. DMA is primarily involved in gas-phase oxidation, wet deposition, and aerosol uptake[46,52]. The main oxidant for amines in the atmosphere is OH, with a reaction rate constant of 6.49×10^{-11} cm^3 mol^{-1} s^{-1} for DMA and OH[53]. The impacts of O_3 and NOx on DMA are minimal, so we only considered the OH oxidation in this study. The Henry's law constant for wet deposition is set at 5.7×10^{-1} mol m^{-3} Pa^{-1}, and the aerosol uptake coefficient for DMA is set at 0.001[34].

We incorporated the H_2SO_4-DMA nucleation mechanism into the WRF-Chem model following the parameterization scheme in previous studies[47,54]. The parameterization scheme for the H_2SO_4-DMA nucleation mechanism incorporated into the model is based on results from the CLOUD (Cosmics Leaving Outdoor Droplets) chamber experiments, primarily involving the variables of H_2SO_4 and DMA. To account for the temperature dependence of the nucleation process, a temperature-dependent function is incorporated into the parameterization scheme. A more detailed explanation of this parameterization scheme can be found in previous studies and references therein[47,54]. We also added other nucleation mechanisms, including binary and ternary neutral and ion-induced nucleation and organic nucleation mechanisms[38,54–56]. The impact of different nucleation mechanisms on PNC and CCN is compared.

In the model, the default Model for Simulating Aerosol Interactions and Chemistry (MOSAIC) aerosol module uses eight size bins to simulate particle size distribution, ranging from 39 nm to 10 μm. The smallest size bin covers diameters from 39 to 78 nm, which is larger than the sizes reported for newly formed particles. As a result, the default eight-bin structure cannot effectively represent the nucleation mode (1–20 nm) and its early growth into larger particles[57,58]. Some studies have improved the capture of nucleation and particle growth processes by reducing the lowest size limit and increasing the number of size bins[36,54,59]. Therefore, this study adjusted the original eight-bin structure by expanding the particle size range from 39 nm – 10 μm to 1 nm – 10 μm and increasing the number of bins to twelve. Although adjusting the size lower limit and increasing the number of bins raises computational costs to some extent, it enhances simulation accuracy. Supplementary Table 2 summarizes the size ranges for each bin in the default 8-bin, adjusted 8-bin, and 12-bin structures. PNC is defined as particles within the size range of 3–1000 nm in this study.

Model applications

The simulation period spans from February 24 to March 18, 2017, with the first five days designated as a spin-up period to minimize the influence of initial conditions on the results, and thus not included in the analysis. The simulation domain is centered in Beijing, covering parts of the Beijing-Tianjin-Hebei region (Supplementary Fig. 13), with a horizontal resolution of 12 km and 44 vertical layers extending from the surface to 50 hPa. The

Yonsei University (YSU) planetary boundary layer scheme was used[60], a method commonly applied in NPF event analysis[14,61,62]. Further details on other physical parameters can be found in Cai et al.[36]. The gas phase chemistry was simulated using the Statewide Air Pollution Research Center (SAPRC-99) mechanism[63], while aerosol chemistry were modeled using the MOSAIC module[33].

The National Centers for Environmental Prediction Final (NCEP FNL) dataset with a resolution of 1.0° × 1.0° was used to provide initial and boundary conditions for the meteorological fields. Anthropogenic emissions data were taken from the Multiresolution Emission Inventory for China (MEIC) version 1.4, featuring a horizontal resolution of 0.25° × 0.25°[64,65]. Biogenic emissions were obtained from the Model of Emissions of Gases and Aerosols from Nature (MEGAN)[66]. Wildfire and biogenic emissions were sourced from the Fire INventory from NCAR (FINN) version 1.5, with a resolution of 1 km[67].

Due to the lack of direct DMA emission inventory, this study established a DMA emission inventory based on the DMA/NH_3 emission ratio source allocation factors proposed by Mao et al.[31]. Specifically, the emissions ratios for agricultural, residential, industrial, transportation, and power plant sources are 0.0015, 0.0100, 0.0018, 0.0009, and 0.0070, respectively. Several studies have confirmed that these ratios significantly improve the model's performance in simulating DMA[34,68,69].

In order to analyze the impact of the H_2SO_4-DMA nucleation mechanism on PNC and CCN, we conducted six simulation scenarios. Three of these scenarios were designed to validate the effects of incorporating the H_2SO_4-DMA nucleation mechanism: one scenario that does not consider any nucleation (sim_no), one that considers only the model's default binary nucleation scenario (sim_default), and one that involves only the H_2SO_4-DMA nucleation mechanism (sim_DMA). The sim_no scenario focuses exclusively on primary emissions. The fourth scenario (sim_all) includes four types of nucleation mechanisms, comparing the influence of H_2SO_4-DMA nucleation with different nucleation mechanisms and primary emissions on PNC and CCN. The remaining two scenarios analyze the impact of DMA sources during the nucleation process, specifically considering agricultural source DMA (sim_agriDMA) and residential source DMA (sim_resiDMA) in the H_2SO_4-DMA nucleation process.

Observation data

The PNSD data from March 1 to 18, 2017, were collected at the Peking University Urban Atmosphere Environment Monitoring Station (PKUERS), located in the northwest of Beijing within the Peking University campus (39°59'21" N, 116°18'25" E). The measurement instruments were placed on the rooftop of a 20-meter-high building. The PNSD data, covering a particle size range from 3 nm to 10 μm, were obtained using a twin differential mobility particle sizer (TDMPS) and an aerodynamic particle sizer (APS, TSI Model 3321). Further details about the observation can be found in previous studies[9,70]. In addition to the PNSD data at the Beijing station, this study also collected air quality and meteorological data for Beijing. Hourly $PM_{2.5}$ and SO_2 concentrations from March 1 to 18, 2017, were downloaded from the website of the China National Environmental Monitoring Center (http://113.108.142.147:20035/emcpublish). Meteorological data were obtained from the National Centers for Environmental Prediction (ftp://ftp.ncdc.noaa.gov/pub/data/noaa/).

Data availability

All the data are available from the corresponding authors upon request.

Code availability

Code sources are available from the corresponding authors upon request.

Received: 3 December 2024; Accepted: 23 March 2025;
Published online: 01 May 2025

References

1. Kerminen, V.-M. et al. Atmospheric new particle formation and growth: review of field observations. *Environ. Res. Lett.* **13**, 103003 (2018).
2. Kulmala, M. et al. Chemistry of atmospheric nucleation: on the recent advances on precursor characterization and atmospheric cluster composition in connection with atmospheric new particle formation. *Annu. Rev. Phys. Chem.* **65**, 21–37 (2014).
3. Ma, N. & Birmili, W. Estimating the contribution of photochemical particle formation to ultrafine particle number averages in an urban atmosphere. *Sci. Total Environ.* **512-513**, 154–166 (2015).
4. Valavanidis, A., Fiotakis, K. & Vlachogianni, T. Airborne Particulate Matter and Human Health: Toxicological Assessment and Importance of Size and Composition of Particles for Oxidative Damage and Carcinogenic Mechanisms. *J. Environ. Sci. Health C Environ. Carcinog. Ecotoxicol. Rev.* **26**, 339–362 (2008).
5. Williamson, C. J. et al. A large source of cloud condensation nuclei from new particle formation in the tropics. *Nature* **574**, 399–403 (2019).
6. Hirshorn, N. S. et al. Seasonal significance of new particle formation impacts on cloud condensation nuclei at a mountaintop location. *Atmos. Chem. Phys.* **22**, 15909–15924 (2022).
7. Merikanto, J., Napari, I., Vehkamäki, H., Anttila, T. & Kulmala, M. New parameterization of sulfuric acid-ammonia-water ternary nucleation rates at tropospheric conditions. *J. Geophys. Res. Atmos.* **112**, D15207 (2007).
8. Ren, J. et al. The NPF Effect on CCN Number Concentrations: A Review and Re-Evaluation of Observations From 35 Sites Worldwide. *Geophys. Res. Lett.* **48**, e2021GL095190 (2021).
9. Guo, S. et al. Elucidating severe urban haze formation in China. *Proc. Natl. Acad. Sci. USA.* **111**, 17373–17378 (2014).
10. Kulmala, M. et al. Is reducing new particle formation a plausible solution to mitigate particulate air pollution in Beijing and other Chinese megacities?. *Faraday Discussions* **226**, 334–347 (2021).
11. Chen, X. et al. Explaining the spatiotemporal variation of fine particle number concentrations over Beijing and surrounding areas in an air quality model with aerosol microphysics. *Environ. Pollut.* **231**, 1302–1313 (2017).
12. Matsui, H. et al. Impact of new particle formation on the concentrations of aerosols and cloud condensation nuclei around Beijing. *J. Geophys. Res. Atmos.* **116**, D19208 (2011).
13. Sun, J. et al. Measurement report: Contribution of atmospheric new particle formation to ultrafine particle concentration, cloud condensation nuclei, and radiative forcing – results from 5-year observations in central Europe. *Atmos. Chem. Phys.* **24**, 10667–10687 (2024).
14. Yu, F. et al. Wintertime new particle formation and its contribution to cloud condensation nuclei in the Northeastern United States. *Atmos. Chem. Phys.* **20**, 2591–2601 (2020).
15. Zhao, B. et al. Formation Process of Particles and Cloud Condensation Nuclei Over the Amazon Rainforest: The Role of Local and Remote New-Particle Formation. *Geophys. Res. Lett*. **49**, e2022GL100940 (2022).
16. Berndt, T., Böge, O., Stratmann, F., Heintzenberg, J. & Kulmala, M. Rapid Formation of Sulfuric Acid Particles at Near-Atmospheric Conditions. *Science* **307**, 698–700 (2005).
17. Kerminen, V. M. et al. Atmospheric nucleation: highlights of the EUCAARI project and future directions. *Atmos. Chem. Phys.* **10**, 10829–10848 (2010).
18. Kulmala, M. How Particles Nucleate and Grow. *Science* **302**, 1000–1001 (2003).
19. Kirkby, J. et al. Role of sulphuric acid, ammonia and galactic cosmic rays in atmospheric aerosol nucleation. *Nature* **476**, 429–433 (2011).
20. Liu, L. et al. Rapid sulfuric acid–dimethylamine nucleation enhanced by nitric acid in polluted regions. *Proc. Natl. Acad. Sci. USA*. **118**, e2108384118 (2021).

21. Bianchi, F. et al. New particle formation in the free troposphere: A question of chemistry and timing. *Science* **352**, 1109–1112 (2016).
22. O'Dowd, C. D. et al. Marine aerosol formation from biogenic iodine emissions. *Nature* **417**, 632–636 (2002).
23. Chen, M. et al. Acid–base chemical reaction model for nucleation rates in the polluted atmospheric boundary layer. *Proc. Natl. Acad. Sci. USA.* **109**, 18713–18718 (2012).
24. Yao, L. et al. Atmospheric new particle formation from sulfuric acid and amines in a Chinese megacity. *Science* **361**, 278–281 (2018).
25. Cai, R. et al. The missing base molecules in atmospheric acid–base nucleation. *Natl. Sci. Rev*. **9**, nwac137 (2022).
26. Huang, X. et al. Comprehensive modelling study on observed new particle formation at the SORPES station in Nanjing, China. *Atmos. Chem. Phys.* **16**, 2477–2492 (2016).
27. Yin, R. et al. Acid–Base Clusters during Atmospheric New Particle Formation in Urban Beijing. *Environ. Sci. Technol.* **55**, 10994–11005 (2021).
28. Ge, X., Wexler, A. S. & Clegg, S. L. Atmospheric amines – Part I. A review. *Atmos. Environ.* **45**, 524–546 (2011).
29. Almeida, J. et al. Molecular understanding of sulphuric acid–amine particle nucleation in the atmosphere. *Nature* **502**, 359–363 (2013).
30. Zheng, J. et al. Measurement of atmospheric amines and ammonia using the high resolution time-of-flight chemical ionization mass spectrometry. *Atmos. Environ.* **102**, 249–259 (2015).
31. Mao, J. et al. High-resolution modeling of gaseous methylamines over a polluted region in China: source-dependent emissions and implications of spatial variations. *Atmos. Chem. Phys.* **18**, 7933–7950 (2018).
32. Chang, Y. et al. Nonagricultural emissions enhance dimethylamine and modulate urban atmospheric nucleation. *Sci. Bull.* **68**, 1447–1455 (2023).
33. Zaveri, R., Easter, R. C., Fast, J. D. & Peters, L. K. Model for Simulating Aerosol Interactions and Chemistry (MOSAIC). *J. Geophys. Res. Atmos.* **113**, D13204 (2008).
34. Li, Y. et al. A dynamic parameterization of sulfuric acid–dimethylamine nucleation and its application in three-dimensional modeling. *Atmos. Chem. Phys.* **23**, 8789–8804 (2023).
35. Birmili, W. & Wiedensohler, A. New particle formation in the continental boundary layer: Meteorological and gas phase parameter influence. *Geophys. Res. Lett.* **27**, 3325–3328 (2000).
36. Cai, C. et al. Incorporation of new particle formation and early growth treatments into WRF/Chem: Model improvement, evaluation, and impacts of anthropogenic aerosols over East Asia. *Atmos. Environ.* **124**, 262–284 (2016).
37. Wu, Z. et al. New particle formation in Beijing, China: Statistical analysis of a 1-year data set. *J. Geophys. Res. Atmos*. **112**, D09209 (2007).
38. Riccobono, F. et al. Oxidation Products of Biogenic Emissions Contribute to Nucleation of Atmospheric Particles. *Science* **344**, 717–721 (2014).
39. Yu, H., Ren, L. & Kanawade, V. P. New Particle Formation and Growth Mechanisms in Highly Polluted Environments. *Curr. Pollution Rep.* **3**, 245–253 (2017).
40. Wang, Z. B. et al. Connection of organics to atmospheric new particle formation and growth at an urban site of Beijing. *Atmos. Environ.* **103**, 7–17 (2015).
41. Chen, X. et al. Improving new particle formation simulation by coupling a volatility-basis set (VBS) organic aerosol module in NAQPMS+APM. *Atmos. Environ.* **204**, 1–11 (2019).
42. Emery, C. A. & Tai, E. Enhanced Meteorological Modeling and Performance Evaluation for Two Texas Ozone Episodes. Final Report Submitted to Texas Natural Resources Conservation Commission, Prepared by ENVIRON International Corporation, Novato (2001).
43. Tesche, T. W., McNally, D. E. & Tremback, C. Operational Evaluation of the MM5 Meteorological Model over the Continental United States: Protocol for Annual and Episodic Evaluation. Prepared for US EPA by Alpine Geophysics, LLC, Ft. Wright, KY, and ATMET, Inc., Boulder (2002).
44. Emery, C. et al. Recommendations on statistics and benchmarks to assess photochemical model performance. *J. Air Waste Manag. Assoc.* **67**, 582–598 (2017).
45. Lai, S. et al. The striking effect of vertical mixing in the planetary boundary layer on new particle formation in the Yangtze River Delta. *Sci. Total Environ.* **829**, 154607 (2022).
46. Yu, F. & Luo, G. Modeling of gaseous methylamines in the global atmosphere: impacts of oxidation and aerosol uptake. *Atmos. Chem. Phys.* **14**, 12455–12464 (2014).
47. Zhao, B. et al. Global variability in atmospheric new particle formation mechanisms. *Nature* **631**, 98–105 (2024).
48. Lai, S. et al. Vigorous New Particle Formation Above Polluted Boundary Layer in the North China Plain. *Geophys. Res. Lett*. **49**, e2022GL100301 (2022).
49. Cai, R. et al. Sulfuric acid–amine nucleation in urban Beijing. *Atmos. Chem. Phys.* **21**, 2457–2468 (2021).
50. Fast, J. D. et al. Evolution of ozone, particulates, and aerosol direct radiative forcing in the vicinity of Houston using a fully coupled meteorology-chemistry-aerosol model. *J. Geophys. Res. Atmos.* **111**, D21305 (2006).
51. Grell, G. et al. Fully coupled "online" chemistry within the WRF model. *Atmos. Environ.* **39**, 6957–6975 (2005).
52. Bergman, T. et al. Geographical and diurnal features of amine-enhanced boundary layer nucleation. *J. Geophys. Res. Atmos.* **120**, 9606–9624 (2015).
53. Carter, W. P. L. Documentation of the SAPRC-99 chemical mechanism for VOC reactivity assessment. Report to the California Air Resources Board, Contracts 92-329 and 95-308 (2000).
54. Zhao, B. et al. Impact of Urban Pollution on Organic-Mediated New-Particle Formation and Particle Number Concentration in the Amazon Rainforest. *Environ. Sci. Technol.* **55**, 4357–4367 (2021).
55. Dunne, E. M. et al. Global atmospheric particle formation from CERN CLOUD measurements. *Science* **354**, 1119–1124 (2016).
56. Wexler, A. S., Lurmann, F. W. & Seinfeld, J. H. Modelling urban and regional aerosols—I. model development. *Atmos. Environ.* **28**, 531–546 (1994).
57. Kulmala, M. et al. Direct Observations of Atmospheric Aerosol Nucleation. *Science* **339**, 943–946 (2013).
58. Kulmala, M. et al. Formation and growth rates of ultrafine atmospheric particles: a review of observations. *J. Aerosol Sci.* **35**, 143–176 (2004).
59. Liu, Y. et al. Strong particle production and condensational growth in the upper troposphere sustained by biogenic VOCs from the canopy of the Amazon Basin. *Atmos. Chem. Phys.* **23**, 251–272 (2023).
60. Hong, S. -Y, Noh, Y & Dudhia, J A New Vertical Diffusion Package with an Explicit Treatment of Entrainment Processes. *Mon. Weather Rev.* **134**, 2318 (2006).
61. Dong, C., Matsui, H., Spak, S., Kalafut-Pettibone, A. & Stanier, C Impacts of New Particle Formation on Short-term Meteorology and Air Quality as Determined by the NPF-explicit WRF-Chem in the Midwestern United States. *Aerosol. Air Quality Res.* **19**, 204–220 (2019).
62. Zhao, B. et al. High concentration of ultrafine particles in the Amazon free troposphere produced by organic new particle formation. *Proc. Natl. Acad. Sci. USA.* **117**, 25344–25351 (2020).
63. Carter, W. P. Implementation of the SAPRC-99 chemical mechanism into the models-3 framework. Report to the United States Environmental Protection Agency (2000).
64. Li, M. et al. Anthropogenic emission inventories in China: a review. *Natl. Sci. Rev.* **4**, 834–866 (2017).
65. Zheng, B. et al. Trends in China's anthropogenic emissions since 2010 as the consequence of clean air actions. *Atmos. Chem. Phys.* **18**, 14095–14111 (2018).
66. Guenther, A. et al. Estimates of global terrestrial isoprene emissions using MEGAN (Model of Emissions of Gases and Aerosols from Nature). *Atmos. Chem. Phys.* **6**, 3181–3210 (2006).

67. Wiedinmyer, C. et al. The Fire INventory from NCAR (FINN): a high resolution global model to estimate the emissions from open burning. *Geosci. Model Dev.* **4**, 625–641 (2011).
68. Ning, A. et al. Overlooked significance of iodic acid in new particle formation in the continental atmosphere. *Proc. Natl. Acad. Sci. USA*. **121**, e2404595121 (2024).
69. Zhang, Q. et al. Contribution of marine biological emissions to gaseous methylamines in the atmosphere: An emission inventory based on multi-source data sets. *Sci. Total Environ.* **898**, 165285 (2023).
70. Tang, L. et al. More Significant Impacts From New Particle Formation on Haze Formation During COVID-19 Lockdown. *Geophys. Res. Lett*. **48**, e2020GL091591 (2021).

Acknowledgements

This study was supported by the Key Research and Development Program project (2022YFC3701000, task 5) and the National Natural Science Foundation of China (42021004).

Author contributions

J.H. conceived the research, Z.F. and J.M. conducted the model development and simulations, L.J. and Y.Q. contributed to data analyses. D.S., S.G., M.H. provided the observation data and result discussions. Z.F. and J.H. wrote the manuscript, and all authors contributed to manuscript editing.

Competing interests

The authors declare no competing interests.

Additional information

Supplementary information The online version contains supplementary material available at https://doi.org/10.1038/s44407-025-00011-y.

Correspondence and requests for materials should be addressed to Jianlin Hu.